



Electron correlation effects at Sn/Si(1 1 1)– 3×3 , $\sqrt{3} \times \sqrt{3}$ and Sn/Ge(1 1 1)– 3×3 , $\sqrt{3} \times \sqrt{3}$ reconstructions

F. Flores^{a,*}, J. Ortega^a, R. Pérez^a, A. Charrier^b,
F. Thibaudau^b, J.-M. Debever^b, J.-M. Themlin^b

^a *Departamento de Física Teórica de la Materia Condensada, Facultad de Ciencias, C-V,
Universidad Autónoma de Madrid, Madrid 28049, Spain*

^b *Groupe de Physique des Etats Condensés, UMR CNRS 6631, Faculté des Sciences de Luminy,
Université de la Méditerranée, Case 901, 13288 Marseille Cedex 9, France*

Abstract

Electron correlation effects for the two-dimensional electron gas associated with the surface bands of the Sn/Si(1 1 1)– 3×3 , $\sqrt{3} \times \sqrt{3}$, Sn/Ge(1 1 1)– 3×3 and $\sqrt{3} \times \sqrt{3}$ reconstructions are analyzed. Unrestricted local-density-approximation (LDA) calculations enable to define a many-body hamiltonian that includes intra- and inter-site electron interactions. From the analysis of this hamiltonian, it can be concluded that the $\sqrt{3} \times \sqrt{3}$ reconstructions present a Mott transition, while the 3×3 surface remains metallic. How these results can be used to discriminate between conflicting models explaining the $\sqrt{3} \times \sqrt{3} \rightarrow 3 \times 3$ phase transition is described. Inverse photoemission data for the Sn/Si(1 1 1) surface suggests that this phase transition can be explained by means of a dynamical fluctuations model. © 2001 Elsevier Science Ltd. All rights reserved.

1. Introduction

The α - $\sqrt{3} \times \sqrt{3}$ reconstruction, induced by the deposition of 1/3 of Sn monolayer on the Ge(1 1 1) surface [1], shows a very intriguing reversible phase transition to a 3×3 reconstruction, when the temperature is lowered from room temperature (RT) to less than, say, 50 K [2,3]. Many different techniques, such as STM, EELS,

* Corresponding author.

E-mail address: fernando@uamc14.fmc.uam.es (F. Flores).

valence-band direct and inverse photoemission, X-rays and core-level spectroscopies, have been used to elucidate the character of this surface phase transition [4–10].

A first model describing the $\sqrt{3} \times \sqrt{3} \rightarrow 3 \times 3$ transition suggested the formation of a charge-density-wave (CDW), due to the two-dimensional Fermi surface nesting [2]. Core-level spectroscopy and valence-band photoemission data, combined with theoretical calculations, were the basis of a dynamical fluctuations model [10], whereby Sn-atoms were assumed to fluctuate at RT between two structurally different sites, forming the $\sqrt{3} \times \sqrt{3}$ geometry, while, at low temperature, Sn-atoms were stabilized in the 3×3 structure. X-ray diffraction shows conflicting evidence, with some results supporting this dynamical fluctuations model [4,9] and other data [5] suggesting that the $\sqrt{3} \times \sqrt{3}$ geometry is rather flat, as assumed in the CDW model [2]. In addition to all this information, Plummer and collaborators [11] have recently shown that defects play a crucial role in the $3 \times 3 \rightarrow \sqrt{3} \times \sqrt{3}$ phase transition, pinning 3×3 domains and operating as nucleation centers.

With all this evidence, there is not yet a full consensus about the character of the $\sqrt{3} \times \sqrt{3}$ structure. While, in some cases, this structure is presented as a flat surface (the CDW model), in the dynamical fluctuations model the $\sqrt{3} \times \sqrt{3}$ surface is contemplated as the average of different 3×3 geometries, which are fluctuating dynamically in a local way.

The aim of this paper is to analyze the electron correlation properties of both the $\sqrt{3} \times \sqrt{3}$ and the 3×3 surfaces for Sn/Ge(1 1 1) and Sn/Si(1 1 1) (this case can be expected to be similar to the previous one [8]), in order to show some crucial differences between the two reconstructions associated with the possible existence of a metal–insulator transition in the surface density of states (DOS). We shall argue that the flat $\sqrt{3} \times \sqrt{3}$ surface should present a Mott transition, while the 3×3 reconstruction remains metallic, even above the transition temperature. This difference between the two geometries could be used as a fingerprint to discriminate between different models, because the flat $\sqrt{3} \times \sqrt{3}$ geometry should be insulating, while the dynamical fluctuation geometry should have a metallic character. Finally, we shall comment on some recent experimental data we have collected and that can be used in this direction.

2. LDA calculations and generalized Hubbard hamiltonian model for surface bands of Sn/Ge(1 1 1) and Sn/Si(1 1 1)

In the first step, we obtained the ground state of the 3×3 and $\sqrt{3} \times \sqrt{3}$ reconstructions using different LDA-codes, and calculated the surface bands associated with each reconstruction. In our theoretical model, the Sn-atoms forming the $\sqrt{3} \times \sqrt{3}$ geometry are located in a T_4 adatom site, as is generally accepted [12,13]. In the $\sqrt{3} \times \sqrt{3}$ case, we force the surface to keep this geometry, while in the 3×3 case the different atoms of the surface are allowed to relax to the total energy minimum, which is found to correspond to a new relaxed 3×3 geometry [13].

For the case of Sn/Ge(1 1 1), we found the 3×3 geometry to be the most stable, with an energy difference with respect to the $\sqrt{3} \times \sqrt{3}$ of less than 10 meV per Sn-

atom [13]. Although these calculations seem to favour the 3×3 reconstruction as the most stable, we stress that its energy difference with the $\sqrt{3} \times \sqrt{3}$ is very small, and we cannot discount the possibility that this difference is within the order of magnitude of the accuracy of the calculations. Moreover, the correlation energy associated with the many-body effects of the surface bands (see below), tends to favour the $\sqrt{3} \times \sqrt{3}$ case by ~ 5 meV per Sn atom, further reducing the energy difference between the 3×3 and the $\sqrt{3} \times \sqrt{3}$ reconstructions. Similar results can be expected for the Sn/Si(111) system. We note, however, that the geometry calculated for the Sn/Ge(111)– 3×3 geometry is in very good agreement with the structural parameters obtained from LEED and X-rays experiments [4,5].

Fig. 1 shows the geometry and the surface bands calculated for the Sn/Si(111) 3×3 reconstruction using the Fireball96 code [14,15]. In these calculations, one Sn-atom per unit cell appears significantly displaced outwards by more than 0.25 \AA with respect to the other two; similar results have been found for the Sn/Ge(111)– 3×3 case [13]. The calculated surface bands (Fig. 1) are readily understood in terms of the reconstructed geometry. The lower band, which accommodates two electrons, is associated with the Sn-atom moving outwards and has more s -character. The two other surface bands, located around E_F , are associated with the two other Sn atoms and have a more pronounced p_z -character.

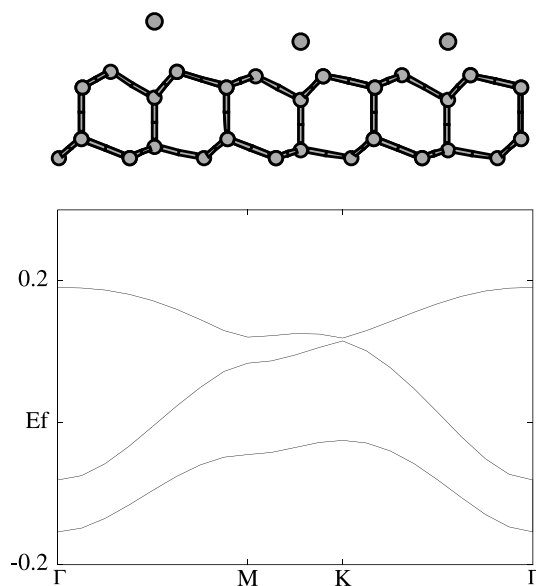


Fig. 1. Atomic geometry (top) and electronic structure (bottom) of Sn/Si(111)– 3×3 surface calculated using Fireball96 code [14,15]. Side view of the unit cell shows three Sn atoms (top atoms) and last four Ge layers. Only three LDA bands closest to Fermi level are displayed along Γ -M, M-K, and K- Γ directions. Lower band, which accommodates two electrons, is associated with upper Sn-atom, while other bands, located around E_F , are associated with other two Sn atoms.

In the second step, we introduce a generalized Hubbard hamiltonian to analyze the many-body effects associated with the surface bands. This hamiltonian reads as follows.

$$\hat{H} = \sum_{\alpha,\sigma} E_{\alpha} \hat{n}_{\alpha\sigma} + \sum_{\alpha \neq \beta, \sigma} t_{\alpha\beta} \hat{c}_{\alpha\sigma}^{\dagger} \hat{c}_{\beta\sigma} + \sum_{\alpha} U_{\alpha} \hat{n}_{\alpha\uparrow} \hat{n}_{\alpha\downarrow} + \frac{1}{2} \sum_{\alpha \neq \beta, \sigma\sigma'} J_{\alpha\beta} \hat{n}_{\alpha\sigma} \hat{n}_{\beta\sigma'}, \quad (2.1)$$

where E_{α} is the energy level of the wave function associated with orbital α ; $t_{\alpha\beta}$ defines the effective hopping between orbitals α and β ; and U_{α} and $J_{\alpha\beta}$ are the on-site ($\alpha\alpha$) and off-sites ($\alpha\beta$) Coulomb interactions. Notice that we only have one orbital (or dangling bond) per site, and that $\hat{n}_{\alpha\sigma}$, $\hat{c}_{\alpha\sigma}^{\dagger}$ and $\hat{c}_{\beta\sigma}$ are the occupation number, creation and annihilation operators, respectively.

Hamiltonian (2.1) has been used as the basic approach to analyze the correlation effects associated with the Sn-dangling bonds. To this end, we fit the different parameters of hamiltonian (2.1) to the electronic surface band properties. Thus, the hopping parameters $t_{\alpha\beta}$ and the effective levels, E_{α}^{eff} , are fitted to the band structure shown in Fig. 1. E_{α}^{eff} includes the initial level, E_{α} , and the Hartree and exchange-correlation potentials. In order to calculate E_{α} , U_{α} and $J_{\alpha\beta}$, we have performed LDA-restricted calculations, changing the occupation number of each of the surface bands of our problem. In [16], we have discussed how to use these calculations to obtain E_{α} and the different Coulomb interaction parameters of hamiltonian (2.1). It should be said that, in this procedure, it is mandatory to have also an LD-solution of hamiltonian (2.1): in this way, we can map out the LDA-restricted calculations of the full crystal onto the LD-solution of hamiltonian (2.1).

Our calculations yield the following approximate values of U_{α} and $J_{\alpha\beta}$, for the Sn/Ge(1 1 1) and Sn/Si(1 1 1) surfaces:

$$\begin{aligned} U(\text{Sn/Ge}) &\simeq 1.1 \text{ eV}, & J_{\text{n.n.}}(\text{Sn/Ge}) &\simeq 0.25 \text{ eV}, \\ U(\text{Sn/Si}) &\simeq 1.5 \text{ eV}, & J_{\text{n.n.}}(\text{Sn/Si}) &\simeq 0.35 \text{ eV}, \end{aligned}$$

where $J_{\text{n.n.}}$ is the Coulomb interaction between nearest-neighbour orbitals.

3. Correlation effects. Metal–insulator transition

Once we have determined its different parameters, we proceed to analyze the properties of hamiltonian (2.1), whose discussion has been published elsewhere [16]. Here, we limit our analysis to presenting general results and a careful comparison between the properties of the 3×3 and $\sqrt{3} \times \sqrt{3}$ reconstructions.

The $\sqrt{3} \times \sqrt{3}$ reconstruction is characterized by having a single orbital and one electron per site and unit cell, which defines a typical half-occupied band with all the sites equivalent. In this particular case, we are interested in the electron local fluctuations appearing between different spins at the same site. In [16] we have shown that, for analyzing these local fluctuations, we can reduce hamiltonian (2.1) to the following Hubbard–hamiltonian:

$$\hat{H}^{(1)} = \sum_{\alpha,\sigma} E_{\alpha} \hat{n}_{\alpha\sigma} + \sum_{\alpha \neq \beta, \sigma} t_{\alpha\beta} \hat{c}_{\alpha\sigma}^{\dagger} \hat{c}_{\beta\sigma} + \sum_{\alpha} U_{\alpha}^{\text{eff}} \hat{n}_{\alpha\uparrow} \hat{n}_{\alpha\downarrow}, \tag{3.1}$$

where $U^{\text{eff}} = U - J_{\text{n.n.}}$, thus, $U_{\alpha}^{\text{eff}}(\text{Sn/Si}) \simeq 1.15 \text{ eV}$ and $U_{\alpha}^{\text{eff}}(\text{Sn/Ge}) \simeq 0.85 \text{ eV}$, which are substantially larger than the corresponding one-electron bandwidth: $W \simeq 0.3 \text{ eV}$ (Sn/Si- $\sqrt{3} \times \sqrt{3}$) and $W \simeq 0.38 \text{ eV}$ (Sn/Ge- $\sqrt{3} \times \sqrt{3}$). This is a case where $U^{\text{eff}} \gg W$ (by, at least, a factor of 2.2), suggesting that the interface should present a Mott transition. Fig. 2 shows, schematically, the physical situation: correlation effects split the surface band into two inequivalent pieces, each one having half of the initial weight.

Next, we consider the 3×3 reconstruction and the corresponding surface bands shown in Fig. 1. We can discuss the main physics of this problem, neglecting the lowest band that is fully occupied with two electrons, and considering only the two partially filled bands associated with the two dangling bonds of the Sn-atoms moving inwards. In this approximation, we find two dangling bonds and a single electron per unit cell. The system, as calculated in LDA, is metallic and we are interested in analyzing its possible metal–insulator transition.

Fig. 3 shows schematically our system, with one electron every second orbital. Can this system present a metal–insulator transition?. The first point to notice about this

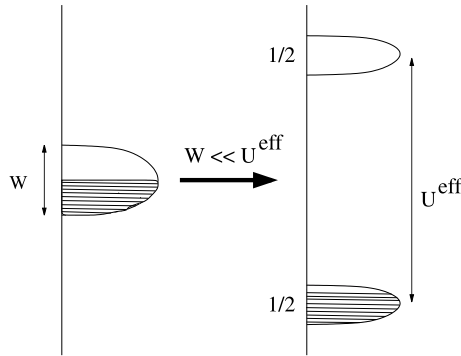


Fig. 2. Metal–insulator transition for $\sqrt{3} \times \sqrt{3}$ reconstruction: correlation effects split half-occupied surface band into two inequivalent pieces, each one having half of initial weight, and system becomes an insulator.

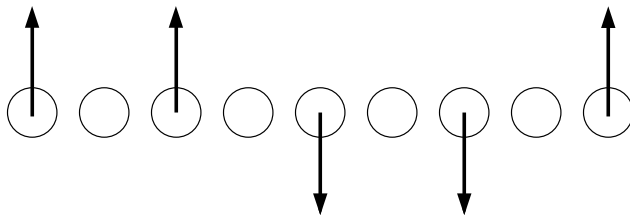


Fig. 3. Metallic LDA solution of 3×3 reconstruction: we find two dangling bond orbitals (associated with two lower Sn atoms) and single electron per unit cell (1/4 occupancy).

case is the following: a local intrasite Coulomb interaction *cannot* create this transition, because, even if U is so large that two electrons cannot be located at the same site simultaneously, the electrons can move along the chain (or the crystal) jumping to an empty site. This shows that a metal–insulator transition can only appear in this “one-quarter” filled band, if the *intersite* Coulomb interaction is large enough to prevent electrons from moving along the crystal.

This discussion shows that an effective hamiltonian, such as that given in (3.1) is not appropriate for analyzing this case. We can introduce, however, the following hamiltonian (see [16]):

$$\hat{H} = \sum_{\alpha,\sigma} E_{\alpha} \hat{n}_{\alpha\sigma} + \sum_{\alpha \neq \beta, \sigma} t_{\alpha\beta} \hat{c}_{\alpha\sigma}^{\dagger} \hat{c}_{\beta\sigma} + \tilde{U}^{\text{eff}} \sum_{\alpha} \hat{n}_{\alpha\uparrow} \hat{n}_{\alpha\downarrow} + \tilde{J}^{\text{eff}} \sum_{\text{n.n.}} \hat{n}_{\alpha} \hat{n}_{\beta}, \quad (3.2)$$

where effective interactions \tilde{U}^{eff} and \tilde{J}^{eff} have been introduced for the intrasite and nearest-neighbour intersite Coulomb interactions. \tilde{U}^{eff} and \tilde{J}^{eff} are given by

$$\begin{aligned} \tilde{U}^{\text{eff}} - \tilde{J}^{\text{eff}} &= U - J_{\text{n.n.}}, \\ \gamma J_{\text{n.n.}} &= (Z - 1) \tilde{J}^{\text{eff}}, \end{aligned}$$

where Z is the lattice coordination number and $(1 + \gamma)J_{\text{n.n.}}$ the Madelung potential created by the charges $n_1 = 1$ and $n_2 = -1$ on the two lattice sites. For the Sn/Si(1 1 1)– 3×3 interface, we obtain the following interactions, $\tilde{J}^{\text{eff}} \simeq 0.25$ eV and $\tilde{U}^{\text{eff}} \simeq 1.40$ eV, while for the Sn/Ge(1 1 1)– 3×3 case $\tilde{J}^{\text{eff}} \simeq 0.2$ eV and $\tilde{U}^{\text{eff}} \simeq 1.05$ eV.

Our analysis of hamiltonian (3.2) shows that a metal–insulator transition can only appear if \tilde{J}^{eff} is larger than the bandwidth, W , associated with the two partially filled bands. In our calculations, W is around 0.27 eV for the Sn/Si(1 1 1)– 3×3 surface and 0.32 eV for the Sn/Ge(1 1 1)– 3×3 case, which shows that we cannot expect to have a metal–insulator phase in these interfaces, although the Sn/Si(1 1 1)– 3×3 is not far from the transition point.

Once we have found that no metal–insulator transition appears in these systems, we analyze their DOS. Without going into details, we show qualitatively in Fig. 4 the kind of DOS we can expect to have, when introducing correlation effects. The local DOS associated with each orbital is only one-quarter filled: the effect of the intrasite Coulomb interaction is to create a new peak, of 1/4th-weight, located at U above E_F . The metallic band is narrowed by 3/4, and 1/4 of electron is still located in this band, which is not deformed too much by the correlation effects.

We conclude by summarizing our results. Due to correlation effects the $\sqrt{3} \times \sqrt{3}$ interfaces show a metal–insulator transition (as found in other cases, such as the SiC(1000)– $\sqrt{3} \times \sqrt{3}$ surface [17,18]), while the 3×3 reconstruction remains metallic.

As mentioned in the introduction, we suggest that this difference between the metallic properties of both reconstructions can be used to discriminate between the different models proposed for the mechanism describing the $\sqrt{3} \times \sqrt{3} \rightarrow 3 \times 3$ transition. The crucial point to notice is the following: if the $\sqrt{3} \times \sqrt{3}$ phase is a mixture of 3×3 equivalent phases, fluctuating between each other, any technique

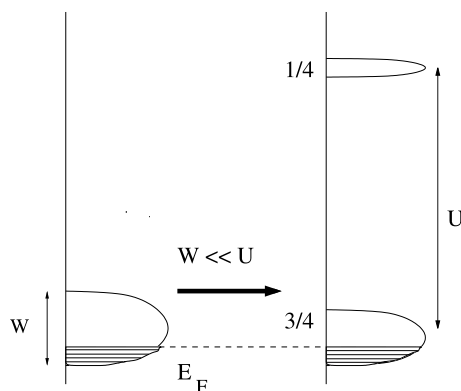


Fig. 4. Correlation effects for 3×3 reconstruction: metallic band is narrowed by $3/4$ and new peak, with $1/4$ weight, is created at $E_F + U$. System remains metallic.

probing its possible insulator character will find a metallic interface. We conclude that this *metallic character will be the fingerprint signalling the validity of the dynamical fluctuations model*.

4. Case of Sn/Si(1 1 1)

We have explored this possibility investigating the Sn/Si(1 1 1)– $\sqrt{3} \times \sqrt{3}$ interface. The advantage of this system is that the defect-induced 3×3 -perturbation at RT has a much shorter spatial extension than in the Sn/Ge(1 1 1) case [8]. Therefore, we can expect the Sn/Si(1 1 1)– $\sqrt{3} \times \sqrt{3}$ reconstruction to be a better test of the validity of the dynamical fluctuations model.

Realizing that the metallic character of the $\sqrt{3} \times \sqrt{3}$ reconstruction, in the fluctuations model, should be combined with a many-body peak above E_F , we have used angle-resolved inverse photoemission spectroscopy to explore the surface states above E_F .

The experiments were performed in two separate ultrahigh vacuum chambers equipped, respectively, with STM and LEED facilities, and the inverse photoemission setup ($h\nu \simeq 9.5$ eV). The preparation of the sample yielded flat areas of nearly perfect $\sqrt{3} \times \sqrt{3}$ reconstructed terraces, with a residual substitutional Si adatom concentration lower than 5%, as estimated by STM (details will be published elsewhere).

Fig. 5 shows the KRIPES spectra for an incident angle $\Theta = 0$, before and after deposition of roughly 1 Langmuir of activated hydrogen. The KRIPES difference curve clearly shows two peaks, U'_1 and U'_2 , which we can associate with the Sn dangling-bond surface states. KRIPES curves for $\Theta \neq 0$ will be published elsewhere, showing that the U'_1 band crosses the Fermi level around the middle of the two-dimensional Brillouin zone.

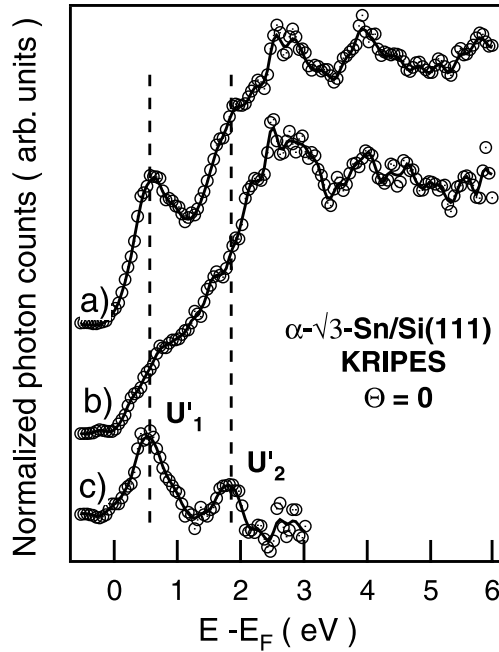


Fig. 5. Normal incidence ($\theta = 0^\circ$) Kripes spectrum of Sn/Si(111)- $\alpha\sqrt{3}$ before (a) and after (b) exposure to roughly 1 Langmuir of atomic hydrogen. (c) Kripes difference curve between (a) and (b) spectra.

These results clearly show: (a) there exists a metallic band at the $\sqrt{3} \times \sqrt{3}$ reconstruction, and (b) a surface state occurs around 1 eV above E_F , which corresponds to the upper correlated band. As discussed above, these results are the fingerprint of the dynamical fluctuations model, as appears to be confirmed by our Kripes-data.

Acknowledgements

This work was funded by the Spanish CICYT under contract PB97-0028.

References

- [1] C.A. Sebenne, in: Fu-Jia, Yang et al. (Ed.), Surface Physics and Related Topics, World Scientific, Singapore, 1991, p. 259.
- [2] J.M. Carpinelli, H.H. Weitering, E.W. Plummer, R. Stumpf, Nature 381 (1996) 398.
- [3] J.M. Carpinelli, H.H. Weitering, M. Bartkowiak, R. Stumpf, E.W. Plummer, Phys. Rev. Lett. 79 (1997) 2859.
- [4] J.Z. Ismail, P.J. Rous, A.P. Baddorf, E.W. Plummer, Phys. Rev. B 60 (1999) 2860.

- [5] O. Bunk, J.H. Zeysing, G. Falkenberg, R.L. Johnson, M. Nielsen, M.M. Nielsen, R. Feidenhans'l, *Phys. Rev. Lett.* 83 (1999) 2226.
- [6] R.I.G. Uhrberg, T. Balasubramanian, *Phys. Rev. Lett.* 81 (1998) 2108.
- [7] A. Goldoni, I. Modesti, *Phys. Rev. Lett.* 79 (1997) 3266.
- [8] L. Ottaviano, M. Crivellari, L. Lozzi, S. Santucci, *Surf. Sci.* 45 (2000) L41.
- [9] T. Yamanaka, S. Ino, *Phys. Rev. B* 61 (2000) R5074.
- [10] J. Avila, A. Mascaraque, E.G. Michel, M.C. Asensio, G. Le Lay, J. Ortega, R. Perez, F. Flores, *Phys. Rev. Lett.* 82 (1999) 442.
- [11] H.H. Weitering, J.M. Carpinelli, A.V. Melechko, J. Zhang, M. Bartkowiak, E.W. Plummer, *Science* 285 (1999) 2107.
- [12] J.E. Northrup, *Phys. Rev. Lett.* 53 (1984) 683.
- [13] J. Ortega, R. Pérez, F. Flores, *J. Phys.: Cond. Matter* 12 (2000) L21.
- [14] O.F. Sankey, D.J. Niklewski, *Phys. Rev. B* 40 (1989) 3979.
- [15] A.A. Demkov, J. Ortega, O.F. Sankey, M.P. Grumbach, *Phys. Rev. B* 52 (1995) 1618.
- [16] F. Flores, J. Ortega, R. Pérez, *Surf. Rev. Lett.* 6 (3&4) (1999).
- [17] J.M. Themlin, et al., *Europhys. Lett.* 39 (1997) 61.
- [18] M. Rohlfing, J. Pollmann, *Phys. Rev. Lett.* 84 (2000) 135.